Published in final edited form as:
Comput Med Imaging Graph. 2012 July ; 36(5): 375–386. doi:10.1016/j.compmedimag.2012.03.005.

MDCT quantification is the dominant parameter in decision–making regarding chest tube drainage for stable patients with traumatic pneumothorax

Wenli Cai[a,*], **June-Goo Lee**[a], **Karim Fikry**[b], **Hiroyuki Yoshida**[a], **Robert Novelline**[a], and **Marc de Moya**[b]

[a]Department of Radiology, Massachusetts General Hospital and Harvard Medical School, USA

[b]Department of Trauma, Emergency Surgery and Surgical Critical Care, Massachusetts General Hospital and Harvard Medical School, USA

Abstract

It is commonly believed that the size of a pneumothorax is an important determinant of treatment decision, in particular regarding whether chest tube drainage (CTD) is required. However, the volumetric quantification of pneumothoraces has not routinely been performed in clinics. In this paper, we introduced an automated computer-aided volumetry (CAV) scheme for quantification of volume of pneumothoraces in chest multi-detect CT (MDCT) images. Moreover, we investigated the impact of accurate volume of pneumothoraces in the improvement of the performance in decision-making regarding CTD in the management of traumatic pneumothoraces. For this purpose, an occurrence frequency map was calculated for quantitative analysis of the importance of each clinical parameter in the decision-making regarding CTD by a computer simulation of decision-making using a genetic algorithm (GA) and a support vector machine (SVM). A total of 14 clinical parameters, including volume of pneumothorax calculated by our CAV scheme, was collected as parameters available for decision-making. The results showed that volume was the dominant parameter in decision-making regarding CTD, with an occurrence frequency value of 1.00. The results also indicated that the inclusion of volume provided the best performance that was statistically significant compared to the other tests in which volume was excluded from the clinical parameters. This study provides the scientific evidence for the application of CAV scheme in MDCT volumetric quantification of pneumothoraces in the management of clinically stable chest trauma patients with traumatic pneumothorax.

Keywords

Computer-aided volumetry (CAV); Computer-aided diagnosis (CAD); Decision-making; Multi-detector computed tomography (MDCT); Pneumothorax; Chest tube drainage

[*]Corresponding author at: Department of Radiology, Massachusetts General Hospital, 25 New Chardon St., 400C, Boston, MA 02114, USA. Tel.: +1 617 726 0515; fax: +1 617 724 6130. Cai.Wenli@mgh.harvard.edu (W. Cai). .

Conflict of interest statement

Wenli Cai, PHD: no financial disclosure, June-Goo Lee, PHD: no financial disclosure, Karim Fikry, MD: no financial disclosure, Hiroyuki Yoshida, PHD: Patent holder, Hologic, Inc; Patent holder, MEDIAN Technologies, Robert Novelline, MD: no financial disclosure, Marc de Moya, MD: no financial disclosure.

1. Introduction

Pneumothorax, a potentially life-threatening condition, is present in 30-39% of patients suffering chest trauma [1-3]. Prompt identification and treatment of traumatic pneumothorax are an imperative part of emergency care for chest trauma patients [4]. Current treatment guidelines, the BTS (British Thoracic Society) [5] and the ACCP (American College of Chest Physicians) [6] guidelines, recommended the treatment of chest tube drainage (CTD) for patients in the presence of clinically unstable conditions and symptoms: such as severe hypoxia, very low blood pressure, or an impaired level of consciousness. These clinically unstable patients tend to be treated before CT imaging or even chest radiography. However, the optimal management of traumatic pneumothoraces for clinically stable patients, i.e. whether to place a chest tube in patients who are otherwise stable, continues to be a contentious issue, considering that the treatment of CTD has a reported complication and failure rate of up to 30% [7-10].

Recent studies observed that the incidence rate of CTD varied from 31% [11] to 67% [12] of injured pneumothorax patients, and up to 82% for patients with concurrent hemothorax [13]. Despite the fact that the size and distribution of overt and occult pneumothoraces are statistically similar [14], 65% of injured patients received a CTD in the case of overt pneumothorax, whereas only 31% underwent CTD when the pneumothorax was occult [11]. Some studies suggest that carefully selected patients may be treated conservatively, ultimately required CTD only in about 10% of cases [15,16]. This large variance in practice reflects the difficulty clinicians have in determining the appropriate treatment for pneumothorax. Overtreatment is particularly important with CTD, as it is associated with an up to 22% rate of major complications [17], including insertional, positional, and infection issues [7,17-19].

It is commonly believed that the size of a pneumothorax is an important determinant of treatment, in particular regarding whether CTD is required [20]. Traditionally, pneumothorax has been diagnosed and its size estimated by use of chest radiography (CXR). A study showed that, by use of an experimental model of pneumothorax, the 2D image analysis on CXR gave a poor estimation of the volume of pneumothorax, regardless of the methods chosen for calculation [21]. With the rapid development of multi-detector CT (MDCT), CT scanning of trauma patients has become the primary method of trauma survey, which provides higher sensitivity and specificity than does either ultrasound or CXR[22,23]. Recently, an automated computer-aided volumetry (CAV) method for quantifying pneumothorax in MDCT images has been developed and evaluated in traumatic patients with occult pneumothorax [24]. However, it is still unclear whether the application of MDCT volumetric quantification of pneumothoraces will tangibly improve the performance in the decision-making regarding CTD.

The purpose in the present study was to investigate whether the MDCT volumetric quantification of pneumothoraces is the dominant clinical parameter in decision-making regarding CTD and thus it may improve the performance in the management of clinically stable patients with traumatic pneumothoraces. For this purpose, we developed an occurrence frequency map that analyzed quantitatively the impact of each clinical parameter in decision-making regarding CTD by use of a computer simulation for decision-making, which employed a genetic algorithm (GA) [25] and a support vector machine (SVM) [26]. By incorporation of the volume of pneumothoraces calculated by our CAV scheme in MDCT images and the diagnostic data collected in a patient trauma survey, the occurrence frequency map quantifies the importance of each clinical parameter in decision-making regarding CTD. Furthermore, the occurrence frequency map provides the scientific evidence

for the application of CAV scheme in MDCT volumetric quantification of pneumothoraces in the management of clinically stable patients with traumatic pneumothorax.

2. Materials and methods

Our institutional review board (IRB) approved this retrospective, HIPAA-compliant study. Informed consent was waived, but patient confidentiality was protected.

2.1. Study patients

Sixty consecutive chest trauma patients who had at least one diagnosed pneumothorax on MDCT were collected for this study at a university level I trauma center from January 2008 to December 2009. The patient inclusion criteria for the study were: (1) chest trauma patients aged ≥18 years were diagnosed with a pneumothorax by CT scan; (2) the patients were not treated by CTD before the acquisition of the chest CT scan. The patient exclusion criteria for the study were as follows: (1) any patient with no CT scan available in our radiology department's information system; (2) any patient who received a chest tube before chest CT scan because of clinical instability.

All subjects were scanned by MDCT scanners (either GE 64-slice or GE 16-slice CT scanner, GE Healthcare, Milwaukee, Wisconsin) with the following parameters: supine position, 120-140 kVp voltage, auto mA tube current setting, 1.25 mm collimation, and 2.5 mm reconstruction interval. A total of 14 clinical parameters that are associated with the CTD decision-making, as described in Table 1, was collected from the original reports, with the exception of the volume that was calculated based on our CAV scheme on MDCT images.

Two trauma surgeons reviewed all collected cases and established the ground truth regarding the decision for CTD in consensus based on the protocol below.

- For patients who were treated by CTD, the clinical cause and the duration of CTD were reviewed. If the output of the chest tube (presence or absence of air leak or fluid output) suggested that the chest tube was necessary, then it was decided that, in fact, the chest tube was necessary. If the chest tube had no output and was removed within the first 24–48 h, CTD was deemed unnecessary.
- In addition, CTD was deemed necessary if the use of a chest tube or the lack of a chest tube changed the oxygenation of the patient, as indicated by pulse oximetry readings or arterial blood gas results, or the patient had an expanding pneumothorax. Otherwise, CTD was deemed unnecessary.

2.2. Computer-aided volumetry of pneumothorax

We developed an automated CAV scheme for quantifying of pneumothoraces in the MDCT images of chest trauma patients [24]. The CAV scheme consisted of four automated steps, as illustrated in Fig. 1, (1) extraction of the pleural region; (2) detection of pneumothoraces; (3) segmentation of the detected pneumothoraces; and (4) volumetry of the segmented pneumothoraces. The CAV scheme was performed in the entire 3D volume of MDCT images.

2.2.1. Extraction of pleural region—The presence of pneumothoraces, contusion, subcutaneous emphysema and streak artifacts on chest trauma MDCT images tend to cause the under-segmentation (missing) and/or oversegmentation (leakage) in the extraction of chest cavity and thus introduces false negatives/positives to the segmentation of pneumothoraces. We applied an automated method named pleural region geometric

modeling (PR-GM) for extraction of the entire pleural region by modeling the pleural surface in MDCT images [27], which uses rib structures as references based on the fact that the pleural cavity is surrounded by the ribs and its surface is very close to the ribs.

Let $I(\boldsymbol{X})$ denote the CT value at a point $\boldsymbol{X} = (x,y,z) \in R^3$ in a CT volume. An axial slab centered at axial slice Z_0 is defined: $\boldsymbol{S}_K(Z_0) = \{I(x,y,z) | Z_0\text{-}K \le z \le Z_0 + K\}$, which encompasses a number of $2K + 1$ consecutive axial slices. $\boldsymbol{S}_K$ sweeps through the entire data volume along axial direction $\boldsymbol{Z}$, as illustrated in Fig. 2(a).

In each axial slab $\boldsymbol{S}_K(Z_0)$, a closest bone projection (CBP) image at axial slice Z_0, $\boldsymbol{S}_K(Z_0)^{CBP}$, is defined as the closest voxel along the direction $\boldsymbol{Z}$ that is above the threshold of bone CT value. If no value above the threshold is found along the direction $\boldsymbol{Z}$ in slab $\boldsymbol{S}_K(Z_0)$, the maximum along direction $\boldsymbol{Z}$ is used for the pixel.

$$S_K(Z_0)^{CBP}(x,y) = \left\{ I\left(x, y, z^{CBP}(x,y)\right) \right\}$$

where

$$z^{CBP}(x,y) = \begin{cases} z|_{\min_{Z_0-K \le z \le Z_0+K}} |z - Z_0| \left(\text{for} \quad I(x,y,z) > I^{Bone}\right); & \text{if} \quad S_K(Z_0)^{MIP}(x,y) \ge I^{Bone} \\ z|I(x,y,z) = S_K(Z_0)^{MIP}(x,y); & otherwise \end{cases}$$

where $S_K(Z_0)^{MIP}(x,y) = \left\{ \max_{Z_0-K \le z \le Z_0+K} I(x,y,z) \right\}$ is the maximum intensity projection (MIP) image of $\boldsymbol{S}_K(Z_0)$, I^{Bone} is the threshold of bone CT value, empirically we set $I^{Bone} = 200$ HU.

Fig. 2(b) shows a CBP image, in which the closest bone points are marked by red color. The inner contours of the ribs were detected by casting rays from the image center to the boundaries. Suppose that the lung is located in the middle of the image in chest CT images. Two centers, the left center (L) and the right center (R), were defined for the left pleural region and the right pleural region, which are estimated using the image size: $L = (1/4Rx, 1/2Ry)$, $R = (3/4Rx, 1/2Ry)$, where Rx, Ry are the image resolution on the axial slice.

We cast a ray from the center (L or R) to every point on the image boundary in the order of $\overrightarrow{LURL}$: left, upper, right and lower, i.e., $x = 1$, $x = Ry$, $x = Rx$, $y = 1$, as shown in Fig. 2(b). If a ray hits a rib, the intersect point that is closest to the image centers along each ray is preserved in the interest rib point set S_L or S_R. A cubic NURBS curve $C^0(t)$ is estimated by least-squares fitting of the interest rib points in each set of S^L and S^R, respectively, by minimizing: $\| \sum_{j=1}^{K} R_{i,3}(t) P_j - S_j \|^2$, where $R_{i,3}(t)$ is the cubic NURBS basic functions and P_j is the control points, S_j is intersect point in S_L or S_R.

To match the curve $C^0(t)$ to the target pleural boundary, points C_i in $C^0(t)$ are updated by searching from the current location along a profile normal to the initial curve $C^0(t)$ within a length I^{CBP}, which is determined by the thickness of $\boldsymbol{S}_K(Z_0)$, i.e., $I^{CBP} = 2K$. To find the update point, we used the following searching function:

$$C_i(t) = \begin{cases} ignore \quad point; & if \quad n_i \cdot g_i < 0 \\ \widehat{C}_i(t); & otherwise \end{cases}$$

where $\boldsymbol{n}_i$ is the normal of the curve, $\boldsymbol{g}_i$ is the local gradient direction, $\hat{C}_1$ is the updated point of which the gradient has the same direction as the curve normal.

Once all points in C^0(t) are updated, an updated curve $C^1(t)$ is generated and the pleural region is extracted using the contour $C^1(t)$ on each axial slice. Both pleural regions estimated by use of the left and right center points are merged. The final pleural region is determined by a region growing within $C^1(t)$ using a threshold of ≤−600 HU on each slice.

Fig. 2(c) and (d) compare the pleural regions extracted by the traditional region growing method using the same threshold of ≤−600 HU (cf. image (c)) and by the developed PR-GM method (cf. Image (d)). It demonstrated that PR-GM method can precisely define the boundaries of the pleural surface, which effectively excludes subcutaneous emphysema that is usually outside the chest cavity.

2.2.2. Detection of pneumothoraces—Because a pneumothorax tends to appear as a homogeneous air pocket between the pleural surface and the lung parenchyma, pneumothorax candidates are defined as contiguous regions of homogeneous air pockets within the pleural region. Two image features, the local mean $\bar{I}(\boldsymbol{X})$ and the standard deviation SD($\boldsymbol{X}$) of CT values at point $\boldsymbol{X}$,

$$\bar{I}(X) = \frac{1}{(2n+1)^3} \sum_{i,j,k=-n}^{n} I(X+(i,j,k)),$$

$$SD(X) = \sqrt{\frac{1}{(2n+1)^3} \sum_{i,j,k=-n}^{n} \left(I(X+(i,j,k)) - \bar{I}(X) \right)^2}$$

are employed in the extracted pleural region for detection of pneumothorax candidates. The window size is set empirically 5 × 5 × 5. We used the following thresholds to detect the homogeneous air pocket:

$$I^{Air} \leq -950 \quad \text{HU} \quad \text{and} \quad SD^{Air} \leq 25$$

This was followed by a 3D connectivity check for detecting the continuous regions of air; i.e., the volume of the air region is larger than a predefined size, such as 0.1 cc. The detected air regions were marked as the pneumothorax candidates, as demonstrated in Fig. 3(b).

2.2.3. Segmentation of pneumothoraces—Pneumothoraces were precisely segmented from the pleural regions by use of our previously developed *dynamic-thresholding level-set* (DTLS) method [28]. The DTLS was initialized by the pneumothoraces detected in the previous step and evolved within the segmented pleural region.

Our DTLS method used multiple speed functions as well as a *shell* structure, which is a thick 3D region encompassing the level set front, and the histogram of the voxel values within the shell for calculating the values of the speed functions [28]. DTLS is evolved by:

$$\frac{\partial \Phi}{\partial t} = -\left(F_A(x) + F_C(x)\right) |\nabla \Phi|;$$

where $F_A(x) = sign(f(x)) \cdot |f(x)|^n$, $f(x) = \begin{cases} 1 & if \quad x<\tau-\Delta \\ \frac{\tau-x}{\Delta} & otherwise \\ -1 & if \quad x>\tau+\Delta \end{cases}$, and

$$F_C(x) = C_{Curvature} \nabla \cdot \left(\frac{\nabla \Phi}{\nabla t} \right).$$

Here, $sign(x)$ is a sign function (a.k.a an indicator), i.e., 1 if x is positive and −1 if x is negative; n is an integer factor that controls the smoothness of the speed of the level set front (we used $n = 2$ for simplicity); τ is a threshold value, determined by Otsu's method [30], that separates the object (foreground) and background in the histogram of the shell. The range, Δ, is set to half of the difference between the threshold and the peak value of the histogram in the shell. F_C is a smoothing term of the shape of the front that is proportional to the mean curvature flow ensuring the numerical stability of the forward-in-time, centered-in-space solution of the partial differential equation [29]. $C_{Curvature}$ is the control parameters smoothing the segmentation results, which was set 0.1 in our study.

During the evolution, the front of the level set was pushed toward the boundary of the pneumothoraces by the optimal threshold calculated from the shell. Fig. 4 demonstrates the process of DTLS on segmentation of a pneumothorax in the right lung in Fig. 3. As a result of segmentation, the medial axis of the shell delineated the boundaries of the pneumothorax, as shown in Fig. 3(c) and (d).

2.2.4. Volumetry of pneumothoraces—The segmented pneumothoraces were grouped into the left and right pleural cavities and thus the volume of pneumothoraces in the left and right pleural cavities were calculated, respectively, as shown in Fig. 5(a), which demonstrates the results of the automated CAV scheme on 3D images. Fig. 5(b) and (c) shows the 3D rendering images of the segmented pneumothoraces and pleural regions in different visualization modes.

This CAV scheme has been validated in an animal study in which the relative difference was 1.66% for the pneumothoraces ≥25 cc and in a patient study in which the relative difference was 7.43% for the pneumothoraces ≥10 cc, and the false-positive rate was, on average, 0.9 per case [24].

2.3. Occurrence frequency map of parameters

We developed an important metrics, *occurrence frequency*, that quantifies the relative importance of individual clinical parameter in decision-making regarding CTD by use of a computer simulation of decision-making that employed a genetic algorithm (GA) [25] and a support vector machine (SVM) [26]. The GA is a stochastic search technique that searches the optimal parameter combination (or 'chromosome' in GA terminology) by maximizing the separation power of a classifier through the possible combinations of clinical parameters based upon the principles of genetic variation and natural selection. Fig. 6 illustrates the process of selecting an optimal parameter combination.

In the context of this study, a parameter combination was modeled as a chromosome or a parameter vector:

$$V = (a_1, \ldots, a_n) \in D^n$$

where a_i is the variable (or "gene" in GA terminology), which has a binary value $a_i \in \{0,1\}$. The search space $D^n \in [0,1]$ was defined as an n-dimensional binary space where 0 and 1 represent the exclusion and inclusion, respectively, of parameter i.

A typical chromosome $\boldsymbol{V}$ may look like 10010101110011, where 1 indicates that the parameter corresponding to a_i is selected for the decision-making regarding CTD; otherwise it is not selected. The decision regarding CTD is binary, i.e., 0 does not need for CTD (conservative solution), 1 needs for CTD (drainage solution). The performance of $\boldsymbol{V}$ was assessed by a fitness function $F(\boldsymbol{V})$ using the parameter combination selected by the chromosome $\boldsymbol{V}$. The fitness value is defined as the area under the receiver operating characteristic (ROC) curve exported by an SVM classifier [26], i.e., the Az value. We employed the leave-one-out cross-validation method [31] to estimate the ROC curve. The leave-one-out method is known to provide an unbiased estimate of the performance of the predictive model that is also more accurate than those of alternative cross-validation or hold-out schemes [31]. The SVM classifier was trained by the selected parameters of all but one case. The trained model was then tested with the case that was excluded for training for calculation of the likelihood of the need for CTD. This procedure was repeated for each case until all available cases have been tested in this manner.

The population size was set to 16 in our GA evolution, i.e., 16 chromosomes $\boldsymbol{V}_1 \ldots \boldsymbol{V}_{16}$ in each generation. The initial population was randomly generated. Then, the corresponding fitness value $F_1 \ldots F_{16}$ were calculated. At each evolution, 8 pairs of chromosomes were mated by the roulette-wheel selection algorithm with the probability of being selected $p_i = F_i / \sum_{j=1}^{16} F_j$. Thus, chromosomes with high fitness values were more likely be selected than that with low fitness values. Once a pair of chromosomes was selected, offspring of the pair were generated by 2-points crossover and 10% mutation probability for genes. The fitness value of each chromosomes in the new population was evaluated and the whole procedure repeated:

Generate random population $\boldsymbol{V}_1 \ldots \boldsymbol{V}_{16}$

REPEAT

evaluate fitness values $F_1 \ldots F_{16}$ of current population by the SVM classifier

select 8 pairs of chromosomes by roulette-wheel selection algorithm

for each pair of chromosomes:

perform 2-points crossover and mutation with 10% probability

to give new improved population

UNTIL finished

The GA and SVM parameters that were used in the study are summarized in Table 2. During the GA evaluation, all of the evaluated chromosomes were saved and sorted based upon their fitness function $F(\boldsymbol{V}_i)$. The top N chromosomes with the largest fitness values were selected as the N-best chromosome set.

The relative importance of an individual parameter (p_i) was assessed by the occurrence frequency of the parameter in the resulting N-best chromosome set [32], which was defined as the likelihood of the parameter selected in the N-best chromosome set,

$$w(p_i) = \frac{\sum_{k=1}^{N} Selected(X_k|p_i)}{N},$$

where N is the number of chromosomes in the N-best chromosome set (N = 100 in our settings), and X_k is one chromosome in the N-best chromosome set. The function Selected($X_k|p_i$) is 1 if the parameter p_i is selected in X_k; otherwise, it is 0. Numerically, $w(p_i)$ ranges from 0.0 to 1.0. A high value of the occurrence frequency indicates that the corresponding parameter is selected frequently in the N-best chromosome set, i.e., it has an important impact on the optimal decision-making.

2.4. Study design

In order to evaluate the importance of the pneumothorax volume on the decision-making regarding CTD, we designed four studies to compare the performances and their associated occurrence frequency maps:

- Study I: with all 14 clinical parameters;
- Study II: with 13 clinical parameters by excluding of the volume;
- Study III: with 11 clinical parameters by excluding of the volume, linear size, and score (because score is calculated from linear size);
- Study IV: with 11 clinical parameters (same as Study III) plus a three-scale size (small, medium, and large) that was visually assessed by two experienced radiologists in consensus on MDCT images.

In these studies, the linear size parameter of a pneumothorax was measured manually on the MDCT images, which was defined as the largest distance in millimeters (mm) between the chest wall and the mediastinal structures along a line perpendicular to the chest wall [33], as demonstrated in Fig. 7(a). The clinical score of a pneumothorax was calculated by addition of 20 to its linear size, if the pneumothorax extended across the pulmonary hilum; otherwise, 10 was added to the linear size [33].

In addition to the occurrence frequency map, the average performance of the 100-best parameter combinations in each study was calculated as the mean performance of the study.

2.5. Data analysis

The statistical analysis was performed with the Stata/SE 10.0 statistical package (Stata Corp. LP, College Station, TX). One-way analysis of variance (ANOVA) was performed for evaluation of the performance of the 100-best parameter combinations in each study. We performed a pairwise F-test for the four studies in order to evaluate whether the variability between each pair of studies was statistically significant. All data analysis was performed with a 95% confidence interval (CI). A p-value of 0.05 or less was considered to indicate statistical significance.

3. Results

Of the 60 subjects, 33 (55%) had left pneumothoraces, 16 (27%) had right pneumothoraces, and 11 (18%) had bilateral pneumothoraces. Thus, a total of 71 pneumothorax cases (counted based on left or right lungs) was diagnosed, including 44 (62%) left pneumothoraces and 27 (38%) right pneumothoraces, of which 21 (30%) were treated by CTD. Most of the pneumothoraces were due to blunt trauma (92%). The mechanism of

injury included motor vehicle collisions ($n = 33$) and falls ($n = 22$). The other 5 were caused by penetrating trauma ($n = 2$), spontaneous pneumothorax ($n = 2$), and prior recent surgery ($n = 1$). The data distributions of the 14 clinical parameters collected are listed in Table 1. The histograms concerning volumes, linear sizes, and visually assessed sizes of the 71 pneumothoraces are shown in Fig. 8.

The occurrence frequency map of the 14 selected clinical parameters in Study I is shown in Fig. 9(a). It indicates that the *Volume* (*cc*) was the dominant clinical parameter for the decision-making concerning CTD. The occurrence frequency value of volume (1.00) was much higher than those for any other clinical parameters. The top five parameters were: Volume (1.00), Heart Rate (0.59), Type (0.48), Score (0.44), and Systolic Blood Pressure (0.37).

The occurrence frequency maps for Studies II, III, and IV are shown in Fig. 9(b, c, and d), respectively. In Study II, after exclusion of volume, linear size emerged as the dominant parameter for decision-making regarding CTD, with an occurrence frequency value of 0.85. After the exclusion of all size parameters (volume, linear size, and score), there were no dominant parameters. Type, Contusion, Position, and PPV became the top four parameters. By addition of the visually assessed three-scale size parameter, the three-scale size became the dominant parameter, with an occurrence frequency value of 1.00.

The performance of the 100-best parameter combinations for the four studies is displayed in Table 3 and Fig. 10. The sizes of the 100-best parameter combinations for four studies are displayed in Table 4. The median size was 4, 5, 7, and 6 for studies I–IV, respectively. This demonstrated that Study I achieved the best performance with the smallest number of parameters, by inclusion of volume. Table 5 shows the p-values from the pairwise F-tests of all studies. The performance between pairs of studies was statistically significantly different, except for the pair of Studies II and IV, which had a p-value of 0.324. Both Study II and Study IV outperformed Study III, indicating that size, even an inaccurate estimation, matters in decision-making regarding CTD. The fact that the difference in the performance between Study II and Study IV was not statistically significant indicated that the linear quantification does not significantly outperform the three-scale visual assessment of the pneumothorax size.

Table 6 lists the best performance with 1, 2, 3, and 4 parameters in Study I. The highest performance with one parameter was 0.899 when volume alone was used, which was slightly below the average performance in Study I (0.905). This indicated that volume alone may not be sufficient for the optimal management of traumatic pneumothorax. However, the performance with volume alone is still above the mean performance of studies II to IV, which did not include volume in the clinical parameters.

Based upon the mean performance in the four studies, we demonstrated that the application of volume (Study I) provided the best performance that was statistically significant compared to the other three studies in which volume was excluded from the clinical parameters. In addition, the size of the 100-best parameter combinations, shown in Table 4, indicated the dominance of the volume of pneumothoraces in decision-making about CTD. Study I had the largest number of the parameter set ($n = 14$), whereas it had the smallest number of parameters in decision-making ($n = 4.39$, 4.39/14 = 31%). In contrast, Study III had the smallest number of the parameter set ($n = 11$), whereas the median size of the best parameter combinations was the largest ($n = 6.66$, 6.66/11 = 61%). The performance of three size parameters alone in the decision-making regarding CTD was compared by the ROC curves and the Az values in Fig. 11. It showed that both volumetric and linear quantification had a better performance than visual assessment, with p-values of 0.0342 (volume vs.

visually assessed three-scale size) and 0.1313 (linear size vs. visual-assessed three-scale size), respectively.

GA provides an efficient way of selecting the parameter combinations with the best performance. An exhaustive method is possible when the number of parameters is not very large. In Study I, the number of possible combinations of 14 clinical parameters was 2^{14}, or 16,384. We finished a test by calculating the performance of all 16,384 parameter combinations. Two occurrence frequency maps, one calculated by the GA, whereas the other calculated by the exhaustive method, were identical when the top 100 best parameter combinations were used. Fig. 12 demonstrates the efficiency of GA's selection of the 100-best parameter combinations. At iteration 90, when less than 9% of the whole combination set was examined, 50% of the 100-best parameter combinations were detected. At iteration 353, GA reached 95% coverage of the 100-best parameter combinations. Considering the fact that we might include more clinical parameters in our future studies, GA is an efficient way for the selection of the best parameter combinations.

4. Discussion

There is much variability in how clinicians make a decision to place a chest tube in patients who are otherwise clinically stable. The 14 clinical parameters collected were meant to include as many factors as possible in the decision-making tree for chest tube placement in stable patients. These were determined after multiple discussions with experts in the field. There are times when clinicians make a decision to place a chest tube on the basis of little information. For example, a blunt trauma patient who is hypotensive for unclear reasons may have a "prophylactic" chest tube placed. In order to eliminate more subjective measures from the cohort of patients, we elected to focus on relatively stable patients who underwent CT scan prior to chest tube placement.

For the optimal management of traumatic pneumothoraces, some studies suggested that it is safe to manage patients with small occult pneumothoraces without CTD [34], whereas some believed that small overt pneumothoraces can be managed likewise without CTD [35]. Some found that not only small, but also moderate-sized traumatic pneumothoraces could be managed without CTD, in the absence of other significant injuries or respiratory compromise[15,36]. Some suggested that occult pneumothorax patients with positive pressure ventilation (PPV) would need CTD [18], whereas some observed that all occult traumatic pneumothoraces could be managed safely without CTD [37]. Although it is commonly believed that the size of a pneumothorax is one of the important factors for initiating treatment of pneumothorax, no volumetric quantification of pneumothoraces was ever performed in the aforementioned studies. Size was generally estimated based upon the linear size or upon visual assessment of a pneumothorax on axial CT images or on CXR.

These aforementioned studies [15,18,34-37] may reflect one view in the management of pneumothoraces. Studies II and IV indicated that linear quantification or visual-size classification plays the dominant role in decision-making about CTD in the absence of volume, which may reflect the observation in the previous studies that a small pneumothorax may be managed without CTD regardless whether its type is occult [34] or overt [35]. Study III indicated that type is one of the major factors when no quantification information is available; this may agree with the observations in refs. [18] and [37]. The observations in refs. [15,36] considered the influence of clinical parameters of RibFx, Systolic BP, HR, and Hct (cf. Table 1) as integrative indictors of patient stability for management of small and medium pneumothorax, as indicated in Study IV.

Clinical parameters may be correlated – for example, linear size and volume. The correlation among parameters may cause them to suppress each other in the selection of the best parameter combinations. For example, the occurrence frequency value of linear size was ranked at the 7th position in Study I, whereas we observed that linear size emerged as the dominant parameter after the excluding of volume from the parameter set (Study II). This indicated that volume and linear size may be correlated, but that the former has more impact on decision-making than does the linear size, and thus it suppresses the importance of linear size in the occurrence frequency map.

The occurrence frequency of a parameter is not an absolute value; rather, it is a relative value for the importance of a parameter within a parameter set in the decision-making. In Study III, because of the lack of dominant parameters, parameters were selected more randomly, and each parameter thus had a similar impact on a decision. Therefore, their occurrence frequencies were higher than those in other studies in which size information was included. For example, the type of pneumothorax had an occurrence frequency value of 0.90 in Study III, whereas it had a value of 0.48, 0.46, and 0.23 in Studies I, II and IV, respectively. This indicates that, when size information was missing, we had to rely on other parameters for decision-making. However, Fig. 10 clearly showed that the performance was significantly lower when size information was missing from the decision-making.

We acknowledge that there were three major limitations in our study. The first limitation was the retrospective nature of the study. The primary decision as to whether to manage a patient with CTD may vary from one surgeon to another according to his/her evaluation of the patient's status. It is difficult to assess the original decisions about CTD. We employed two trauma surgeons to review the decisions about CTD retrospectively, and we established the ground truth in their consensus to minimize the uncertainty regarding the decision-making. We understand that a prospective study might be ideal for this purpose; however, it is very difficult in practice to obtain informed consent from traumatized patients. This retrospective manner limited our study. We emphasize that, although our computer simulation is not an ideal replica of the decision-making of trauma surgeons, it provides a good approximation to the process of decision-making.

Another limitation was that our study population was limited to relatively stable chest trauma patients for whom we had MDCT scanning before CTD. The requirement of MDCT prior to CTD excluded the clinically unstable patients who had CTD before CT imaging (severe patients), and asymptomatic patients with small pneumothorax who did not undergo CT imaging (mild patients) from our study. Clinical guidelines recommend immediate treatment of CTD for clinically unstable pneumothorax patients and thus before CT imaging. In addition, because of the MDCT, a large portion of the pneumothoraces in our study was occult pneumothorax (73%). This limitation might introduce potential bias to the conclusion. However, it is a clinical consensus that severe pneumothorax patients need immediate treatment, whereas it is safe to manage mild pneumothorax patients without CTD. The lack of consensus is the optimal management for moderate pneumothorax patients who are otherwise clinically stable. The results of our study is limited to this patient cohort.

The third limitation of the study was that the 11 patients with bilateral pneumothoraces were evaluated individually as having 22 separate pneumothoraces, which may cause statistical bias. We understand that a patient with bilateral pneumothoraces is likely to have drainage even though the total volume of the pneumothoraces is similar to that of unilateral pneumothoraces. Because the drainage is applied to each lung separately, a bilateral pneumothorax patient may be drained on one side of the lung and the other side of the lung remains untreated. This will cause the decision-making regarding CTD to involve two quantification data: the size of the pneumothoraces in both lungs as well as the size of the

pneumothoraces in each lung. To simplify the context of the computer simulation of the decision-making, we considered the decision of drainage to each side of the lung separately in the case of bilateral pneumothorax. In addition, the bias caused was minimized so that both trauma surgeons who reviewed all cases and established the ground truth were informed to treat the bilateral pneumothoraces cases as unilateral pneumothoraces in making their decisions.

In conclusion, our study demonstrated that MDCT quantification of pneumothoraces has a more important impact on the decision-making regarding CTD than do other clinical parameters in the management of traumatic pneumothorax for patients who are clinically stable. The application of accurate volumes of pneumothoraces has the potential tangibly to improve the performance of the decision-making regarding CTD. We understand that the establishment of a volume-based clinical guideline for pneumothorax management is a difficult task and requires the involvement and consensus of the whole community, which is far beyond the scope of this study. Nevertheless, this study provides the scientific evidence for the application of volumetric quantification in the management of traumatic pneumothoraces in clinical practice.

Acknowledgments

This research was conducted with the support of grant number 1 UL1 RR025758-01, Harvard Clinical and Translational Science Center, from the National Center for Research Resources.

Biography

Wenli Cai, PhD, Assistant Professor of Radiology at Harvard Medical School and attending computer scientist in the Department of Radiology at Massachusetts General Hospital. His research interests are 3D imaging and medical image processing.

June-Goo Lee, PhD, Research Fellow in the Department of Radiology at Massachusetts General Hospital and Harvard Medical School. His research interest is computer-aided diagnosis.

Karim Fikry, MD, Clinical Fellow in the Department of Trauma, Emergency Surgery and Surgical Critical Care at Massachusetts General Hospital and Harvard Medical School. His research interest is emergency surgery.

Hiroyuki Yoshida, PhD, Associate Professor of Radiology at Harvard Medical School and director of the 3D Research Laboratory in the Department of Radiology at Massachusetts General Hospital. His research interests are computer-aided diagnosis and medical image analysis.

Robert Novelline, MD, Professor of Radiology at Harvard Medical School and Director of the Division of Emergency Radiology at Massachusetts General Hospital. His research interests are emergency radiology and radiology education.

Marc de Moya, MD, Assistant Professor of Surgery at Harvard Medical School and attending surgeon in the Department of Trauma, Emergency Surgery and Surgical Critical Care at Massachusetts General Hospital. His research interests are trauma and non-trauma surgery for patients who require acute care.

References

[1]. Shorr RM, Crittenden M, Indeck M, Hartunian SL, Rodriguez A. Blunt thoracic trauma. Analysis of 515 patients. Ann Surg. 1987; 206:200–5. [PubMed: 3606246]

[2]. Tekinbas C, Eroglu A, Kurkcuoglu IC, Turkyilmaz A, Yekeler E, Karaoglanoglu N. Chest trauma: analysis of 592 cases. Ulus Travma Acil Cerrahi Derg. 2003; 9:275–80. [PubMed: 14569484]

[3]. Farooq U, Raza W, Zia N, Hanif M, Khan MM. Classification and management of chest trauma. J Coll Phys Surg Pak. 2006; 16:101–3.

[4]. Ryan B. Pneumothorax: assessment and diagnostic testing. J Cardiovasc Nurs. 2005; 20:251–3. [PubMed: 16000911]

[5]. Henry M, Arnold T, Harvey J. Pleural Diseases Group, Standards of Care Committee, British Thoracic Society. BTS guidelines for the management of spontaneous pneumothorax. Thorax. 2003; 58(Suppl. 2):ii39–52. [PubMed: 12728149]

[6]. Baumann MH, Strange C, Heffner JE, Light R, Kirby TJ, Klein J, et al. Management of spontaneous pneumothorax: an American College of Chest Physicians Delphi consensus statement. Chest. 2001; 119:590–602. [PubMed: 11171742]

[7]. Bailey RC. Complications of tube thoracostomy in trauma. J Accid Emerg Med. 2000; 17:111–4. [PubMed: 10718232]

[8]. Horsley A, Jones L, White J, Henry M. Efficacy and complications of small-bore, wire-guided chest drains. Chest. 2006; 130:1857–63. [PubMed: 17167009]

[9]. Maskell NA, Medford A, Gleeson FV. Seldinger chest drain insertion: simpler but not necessarily safer. Thorax. 2010; 65:5–6. [PubMed: 20029035]

[10]. Chan L, Reilly KM, Henderson C, Kahn F, Salluzzo RF. Complication rates of tube thoracostomy. Am J Emerg Med. 1997; 15:368–70. [PubMed: 9217527]

[11]. Ball CG, Kirkpatrick AW, Laupland KB, Fox DI, Nicolaou S, Anderson IB, et al. Incidence, risk factors, and outcomes for occult pneumothoraces in victims of major trauma. J Trauma. 2005; 59:917–24. discussion 924-5. [PubMed: 16374282]

[12]. Neff MA, Monk JS Jr, Peters K, Nikhilesh A. Detection of occult pneumothoraces on abdominal computed tomographic scans in trauma patients. J Trauma. 2000; 49:281–5. [PubMed: 10963540]

[13]. Stafford RE, Linn J, Washington L. Incidence and management of occult hemothoraces. Am J Surg. 2006; 192:722–6. [PubMed: 17161082]

[14]. Ball CG, Kirkpatrick AW, Laupland KB, Fox DL, Litvinchuk S, Dyer DM, et al. Factors related to the failure of radiographic recognition of occult posttraumatic pneumothoraces. Am J Surg. 2005; 189:541–6. discussion 546. [PubMed: 15862493]

[15]. Johnson G. Traumatic pneumothorax: is a chest drain always necessary? J Accid Emerg Med. 1996; 13:173–4. [PubMed: 8733651]

[16]. Plurad D, Green D, Demetriades D, Rhee P. The increasing use of chest computed tomography for trauma: is it being overutilized? J Trauma. 2007; 62:631–5. [PubMed: 17414339]

[17]. Ball CG, Lord J, Laupland KB, Gmora S, Mulloy RH, Ng AK, et al. Chest tube complications: how well are we training our residents? Can J Surg. 2007; 50:450–8. [PubMed: 18053373]

[18]. Enderson BL, Abdalla R, Frame SB, Casey MT, Gould H, Maull KI. Tube thoracostomy for occult pneumothorax: a prospective randomized study of its use. J Trauma. 1993; 35:726–9. discussion 729-30. [PubMed: 8230337]

[19]. Etoch SW, Bar-Natan MF, Miller FB, Richardson JD. Tube thoracostomy. Factors related to complications. Arch Surg. 1995; 130:521–5. discussion 525-6. [PubMed: 7748091]

[20]. Cameron, P. Textbook of adult emergency medicine. Churchill Livingstone; New York/ Edinburg: 2000.

[21]. Engdahl O, Toft T, Boe J. Chest radiograph—a poor method for determining the size of a pneumothorax. Chest. 1993; 103:26–9. [PubMed: 8417891]

[22]. Kanz KG, Körner M, Linsenmaier U, Kay MV, Huber-Wagner SM, Kreimeier U, et al. Priority-oriented shock trauma room management with the integration of multiple-view spiral computed tomography. Unfallchirurg. 2004; 107:937–44. [PubMed: 15452654]

[23]. Huber-Wagner S, Lefering R, Qvick LM, Körner M, Kay MV, Pfeifer KJ, et al. Effect of whole-body CT during trauma resuscitation on survival: a retrospective, multicentre study. Lancet. 2009; 373:1455–61. [PubMed: 19321199]

[24]. Cai W, Tabbara M, Takata N, Yoshida H, Harris GJ, Novelline RA, et al. MDCT for automated detection and measurement of pneumothoraces in trauma patients. AJR Am J Roentgenol. 2009; 192:830–6. [PubMed: 19234283]

[25]. Goldberg, GE. Genetic algorithms in search, optimization, and machine learning. Addison-Wesley; Reading, MA: 1989.

[26]. Vapnik, VN. The nature of statistical learning theory. 2nd ed.. Vol. xix. Springer; New York: 2000. p. 314

[27]. Cai W, Lee EY, Vij A, Mahmood SA, Yoshida H. MDCT for computerized volumetry of pneumothoraces in pediatric patients. Acad Radiol. 2011; 18:315–23. [PubMed: 21216160]

[28]. Cai W, Holalkere N, Harris G, Sahani D, Yoshida H. Dynamic-threshold level set method for volumetry of porcine kidney in CT images: in vivo and ex vivo assessment of the accuracy of volume measurement. Acad Radiol. 2007; 14:890–6. [PubMed: 17574138]

[29]. Ho, S.; Bullitt, E.; Gerig, G. Level set evolution with region competition: automatic 3-D segmentation of brain tumors; Proceedings of 16th International Conference on Pattern Recognition; 2002. p. 532-5.

[30]. Otsu N. A threshold selection method from gray level histograms. IEEE Trans Syst Man Cybern. 1979; 9:62–6.

[31]. Li Q, Doi K. Comparison of typical evaluation methods for computer-aided diagnostic schemes: Monte Carlo simulation study. Med Phys. 2007; 34:871–6. [PubMed: 17441232]

[32]. Zhang B, Horvath S. Ridge regression based hybrid genetic algorithms for multilocus quantitative trait mapping. Int J Bioinform Res Appl. 2005; 1:261–72. [PubMed: 18048135]

[33]. de Moya MA, Seaver C, Spaniolas K, Inaba K, Nguyen M, Veltman Y, et al. Occult pneumothorax in trauma patients: development of an objective scoring system. J Trauma. 2007; 63:13–7. [PubMed: 17622863]

[34]. Garramone RR Jr, Jacobs LM, Sahdev P. An objective method to measure and manage occult pneumothorax. Surg Gynecol Obstet. 1991; 173:257–61. [PubMed: 1925893]

[35]. Hill SL, Edmisten T, Holtzman G, Wright A. The occult pneumothorax: an increasing diagnostic entity in trauma. Am Surg. 1999; 65:254–8. [PubMed: 10075304]

[36]. Symington L, McGugan E. Towards evidence based emergency medicine: best BETs from the Manchester Royal Infirmary. Bet 1: is a chest drain necessary in stable patients with traumatic pneumothorax? Emerg Med J. 2008; 25:439–40. [PubMed: 18573962]

[37]. Wilson H, Ellsmere J, Tallon J, Kirkpatrick A. Occult pneumothorax in the blunt trauma patient: tube thoracostomy or observation? Injury. 2009; 40:928–31. [PubMed: 19539280]

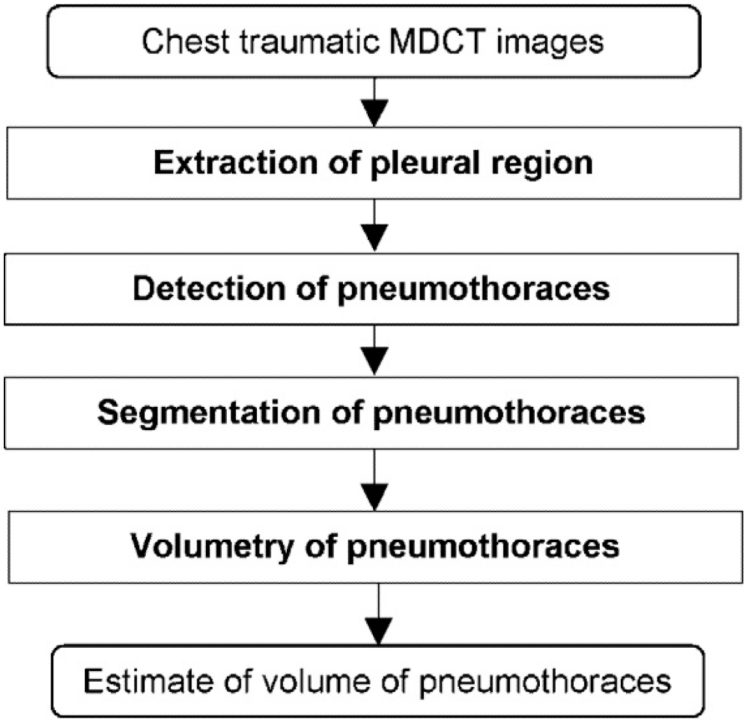

Fig. 1.
Diagram of the computer-aided volumetry (CAV) scheme for automated volumetric quantification of pneumothoraces.

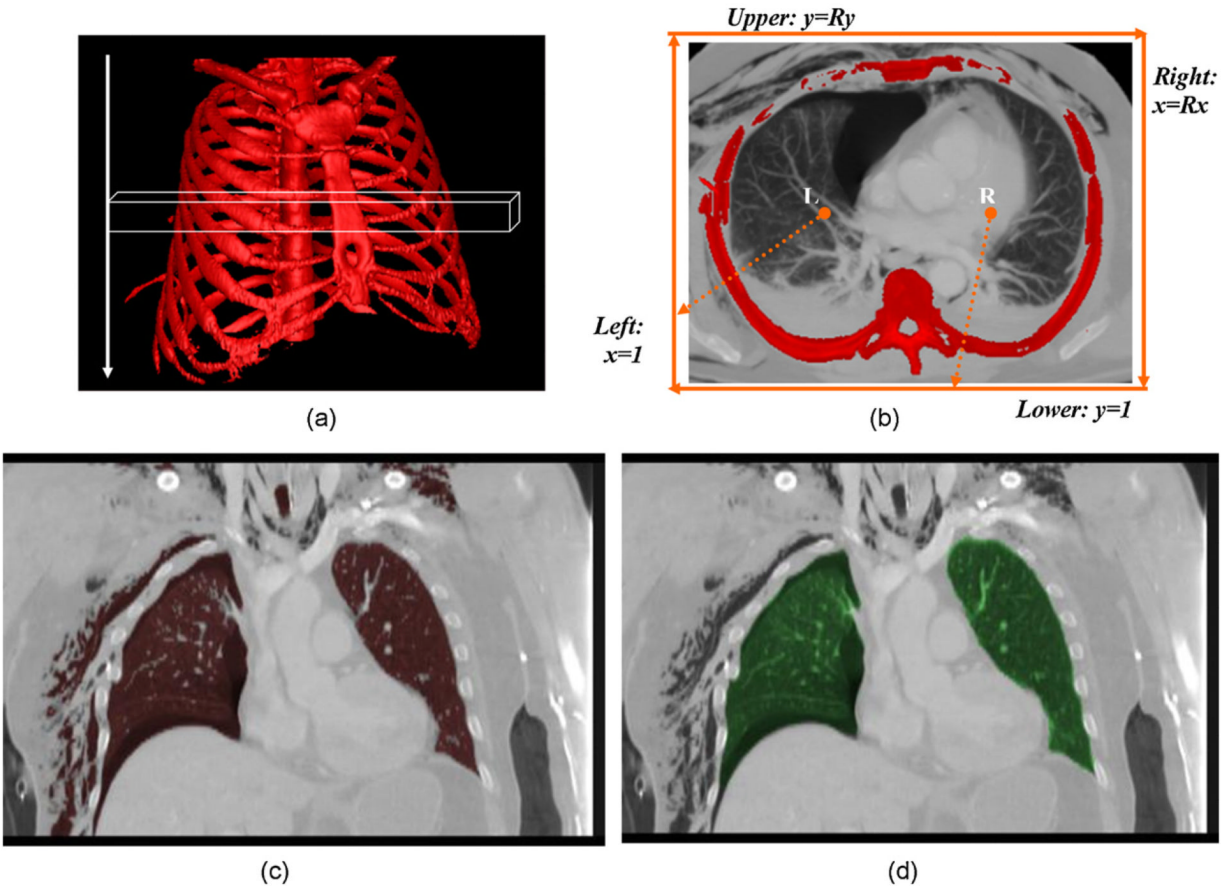

Fig. 2.

Illustration of pleural region geometric modeling (PR-GM) method for extraction of the pleural region by modeling the pleural surface in CT images. (a) An axial slab structure. (b) A closest bone projection (CBP) image: the contour of pleural surface is estimated using the rib locations on the CBP image. (c) Traditional region growing method (e.g. threshold of −600 HU) tends to introduce leakages, such as caused by the subcutaneous emphysema. (d) PR-GM method can effectively exclude subcutaneous emphysema.

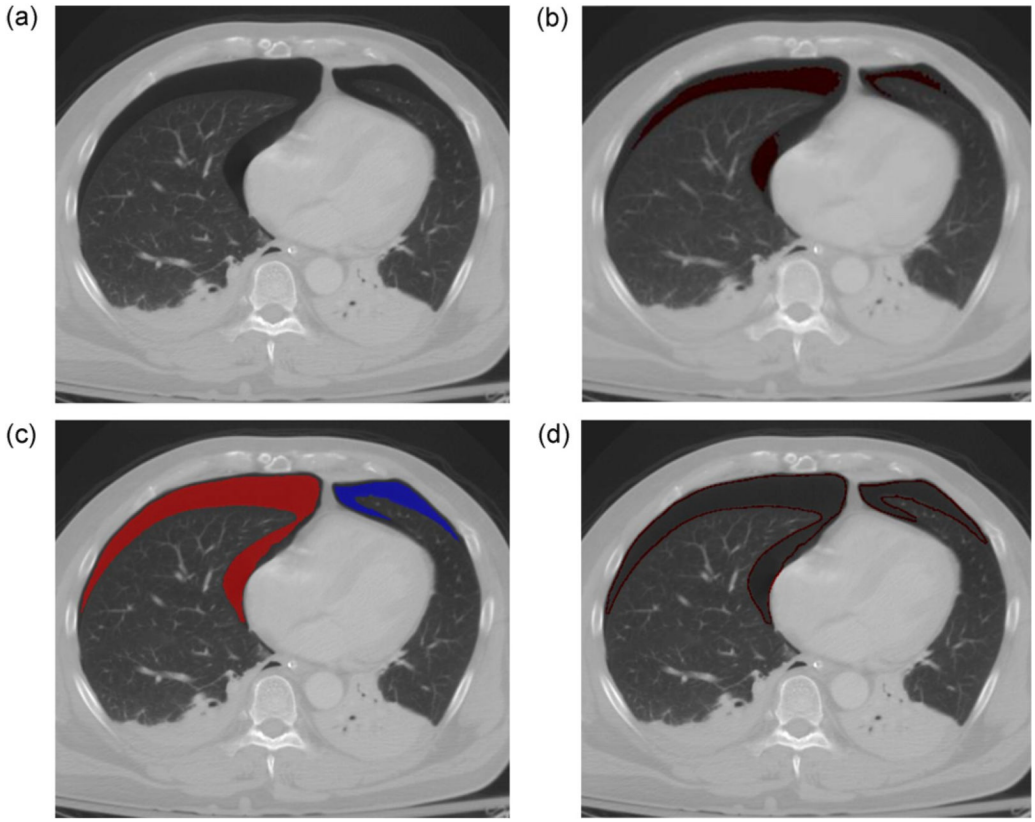

Fig. 3.
The detection and segmentation of pneumothoraces. (a) One axial slice of chest CT scan. (b) The homogeneous air regions were detected as the pneumothorax candidates. (c) Pneumothorax candidates were segmented by dynamic-threshold level-set method. (d) Contours of the segmented pneumothoraces.

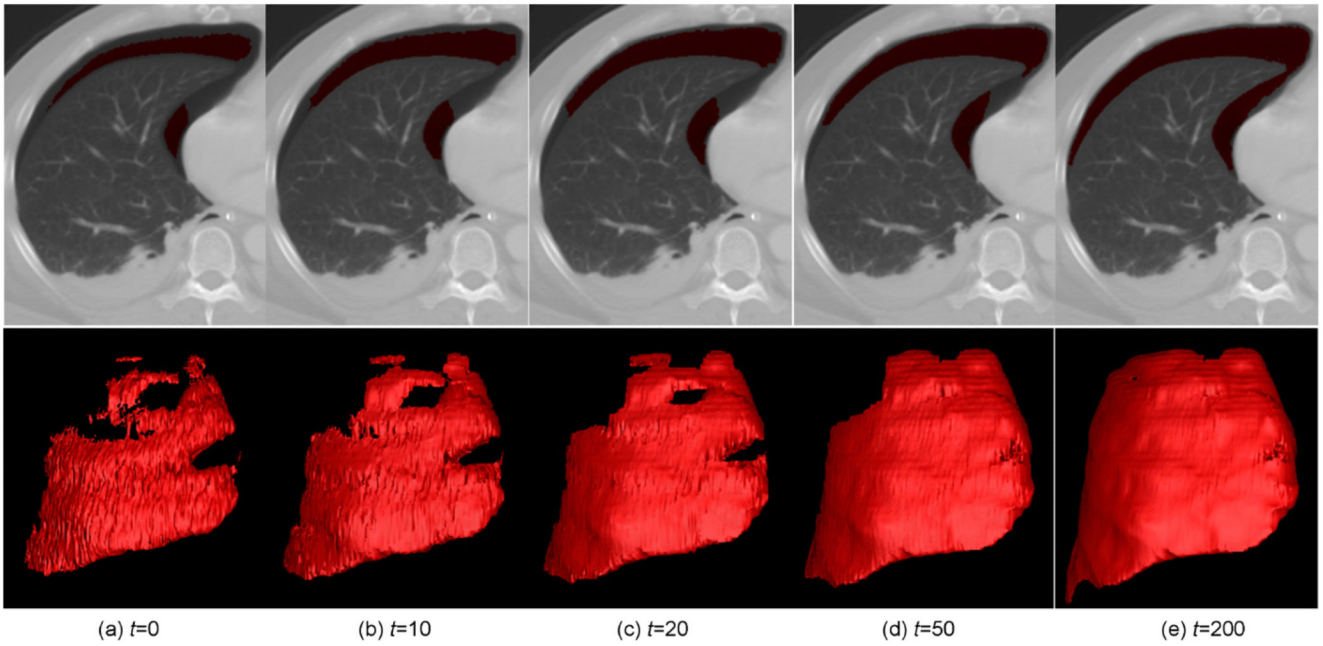

Fig. 4.

Illustration of the 3D segmentation process of a pneumothorax in the right lung in Fig. 3. Upper row is 2D snapshots and lower row is 3D snapshots taken during the evolution of DT level set. (a) Initialization by detected seed region, (b)–(e) are results after 10, 20, 50, and 200 loops of evolution, respectively. The resulting threshold was −875 HU.

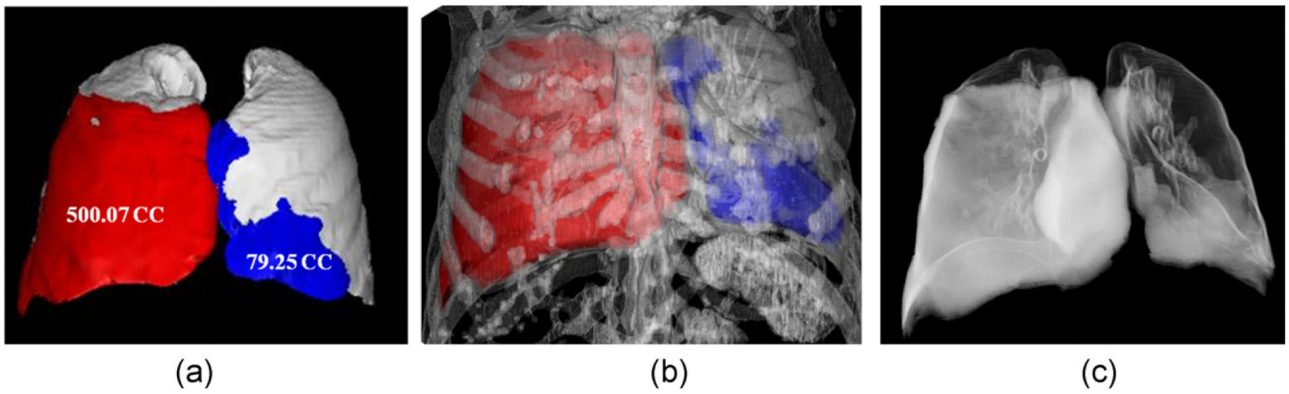

Fig. 5.
Volumetry and visualization of pneumothoraces (a) 3D-rendering images of segmented pleural regions and volumetry of pneumothoraces. (b) 3D-rendering images of MDCT data with the segmented pneumothoraces. (c) The segmented pneumothoraces were rendered with segmented pleural regions by the X-ray model.

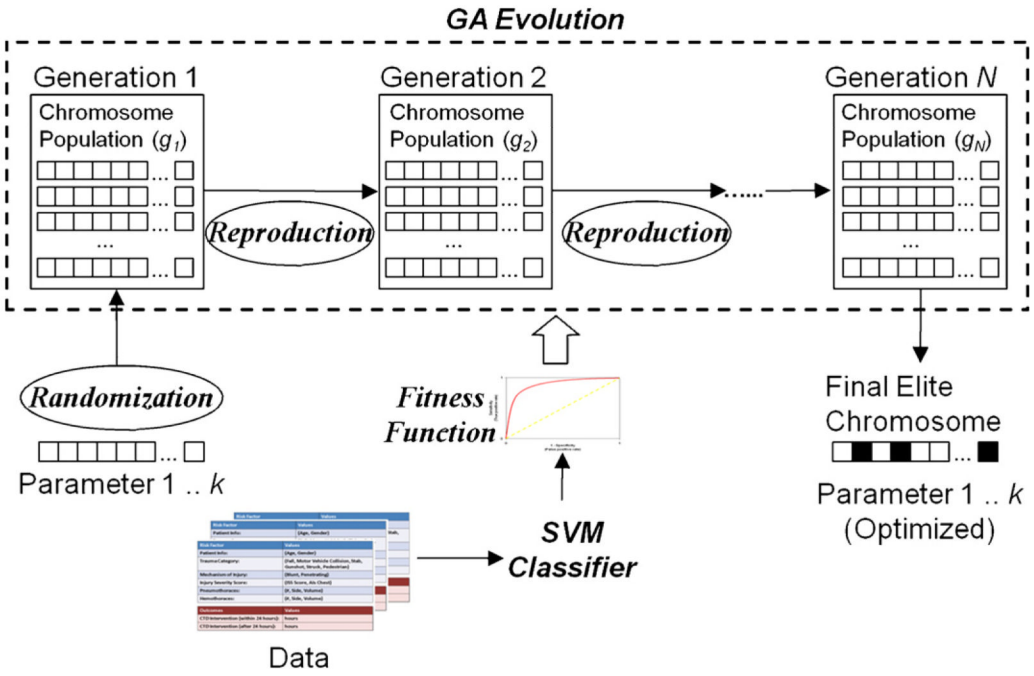

Fig. 6.

Illustration of the application of a genetic algorithm (GA) and a support vector machine (SVM) to the selection of the optimal parameter combination.

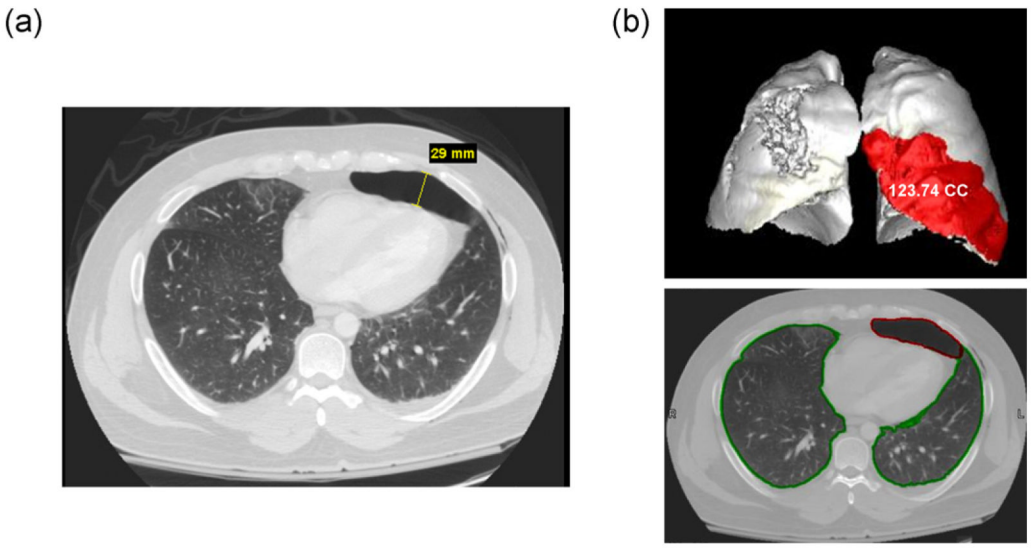

Fig. 7.
Illustration of the two quantification methods for pneumothorax on a 31-year-old/male chest trauma patient. (a) The linear size of the pneumothorax was measured manually as the largest distance (29 mm) between the chest wall and the mediastinal structure along a line perpendicular to the chest wall. (b) The volumetric size of the pneumothorax was measured as the volume (123.74 cc) by our automated computer-aided volumetry (CAV) scheme for pneumothorax. (refer to the red color). (For interpretation of the references to color in this figure legend, the reader is referred to the web version of the article.)

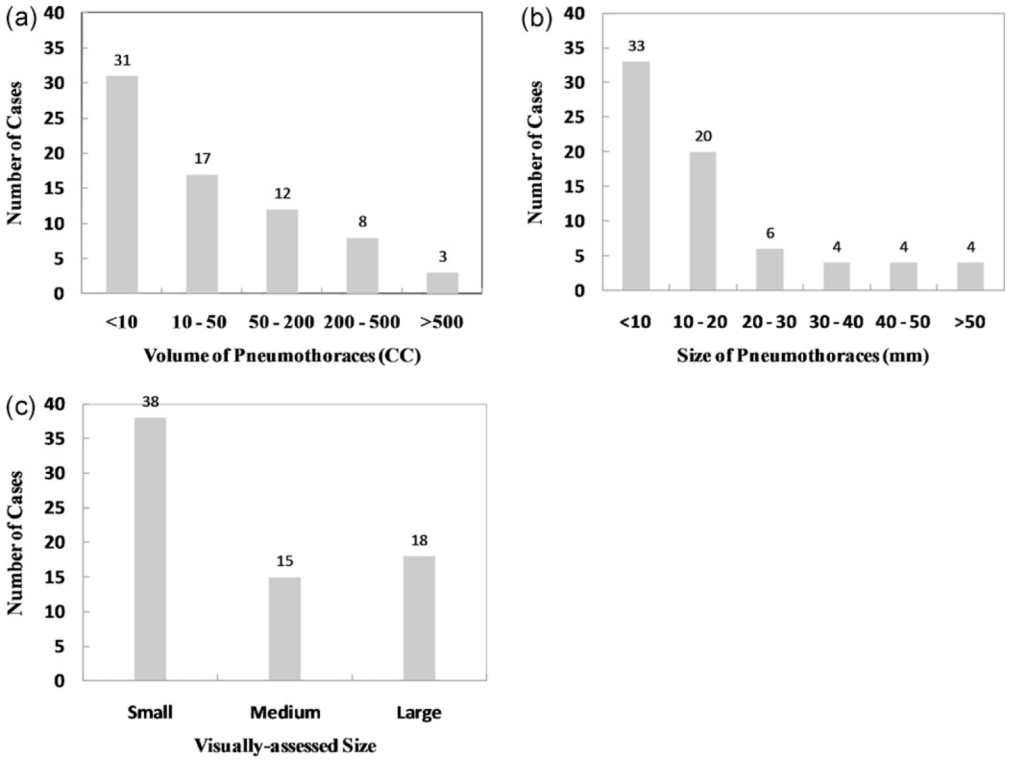

Fig. 8.

Distributions of volume, linear size, and visually assessed size of the 71 pneumothoraces in the study. (a) Histogram of the volumes of the pneumothoraces. (b) Histogram of the linear size of the pneumothoraces. (c) Histogram of the visually assessed size of the pneumothoraces.

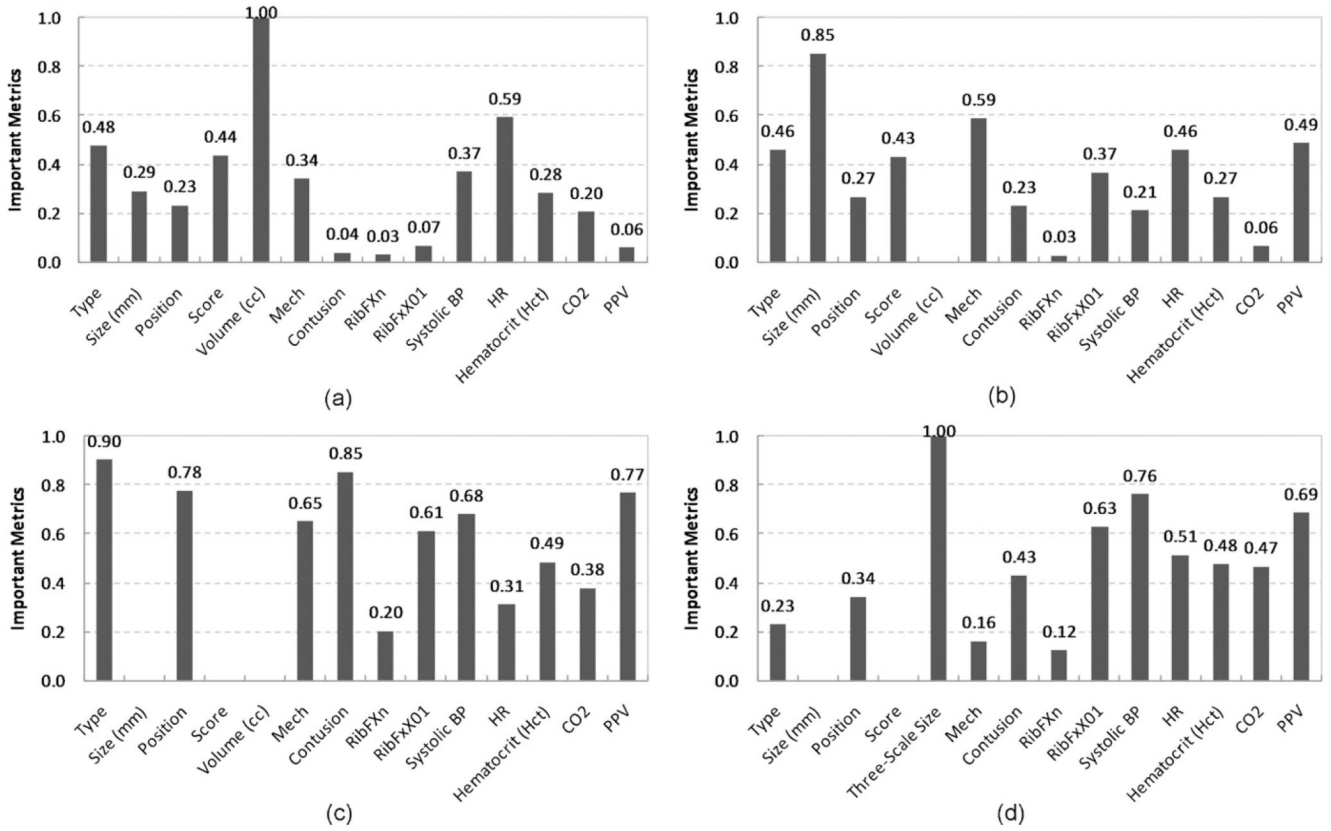

Fig. 9.

Occurrence frequency maps of clinical parameters that were generated by 100-best parameter combinations, or chromosomes, selected by GA. An occurrence frequency value of 1.0 for a parameter indicates that the parameter was always selected for the classifier, whereas 0.0 indicates that the parameter was never selected. (a) Study I: all 14 parameters. (b) Study II: 13 parameters, without volume. (c) Study III: 11 parameters, without size information (i.e. without size, score, and volume). (d) Study IV: 11 parameters plus three-scale size (small, medium, large).

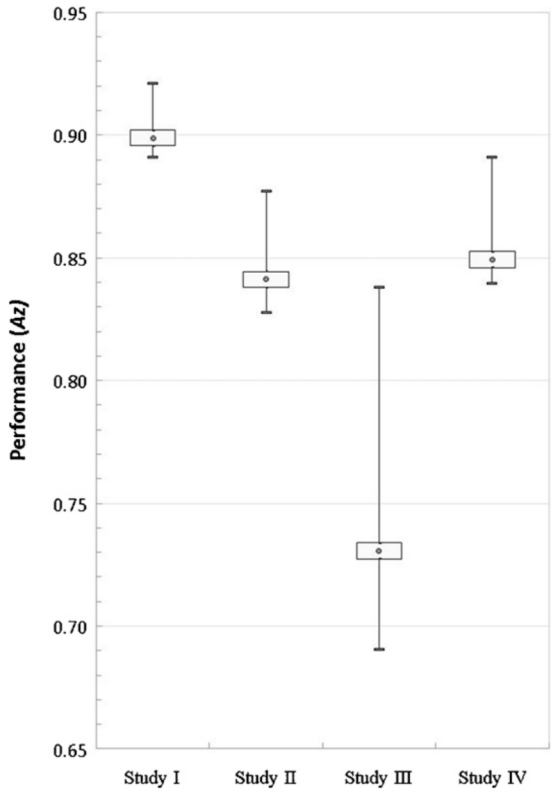

Fig. 10.

Performance of the four studies. The high/low lines indicate the maxima and minima of the *Az* values. The box indicates the range of *Az* in 95% CI, in which the dot is the mean value.

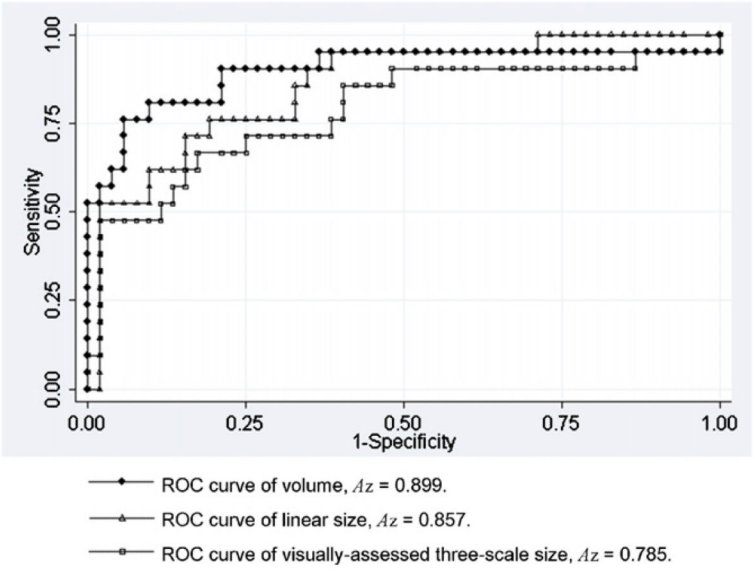

Fig. 11.

Comparisons among three receiver operating characteristic (ROC) curves of volume, linear size, and visually assessed three-scale size in predicating the need for CTD. The areas under the ROC curve (Az) were 0.899 (volume), 0.857 (linear size), and 0.785 (visually assessed three-scale size), respectively.

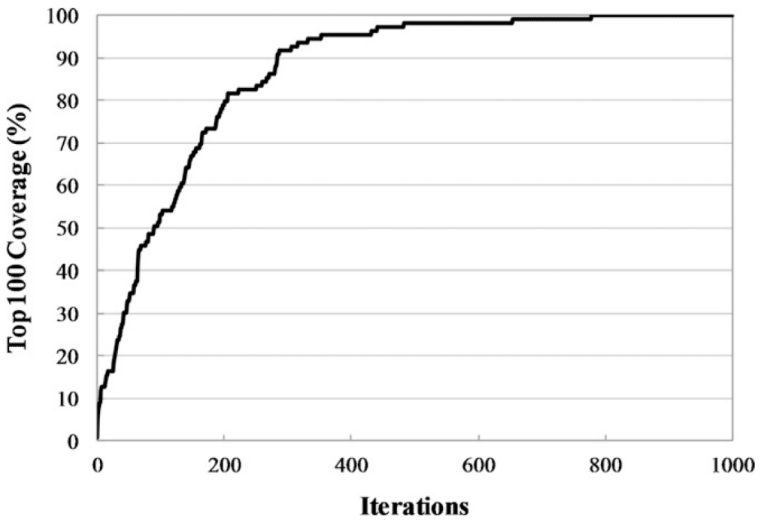

Fig. 12.

The efficiency of the GA's selection of the top 100 best parameter combinations in Study I. The total number of possible parameter combination is 2^{14}, which is 16,384. The population at each iteration (generation) is 16. At iteration 90, when the GA had examined less than 9% of the whole combinations, 50% of the top 100 best parameter combinations were detected. At iteration 353, GA reaches 95% coverage of the top 100 best parameter combinations.

Comput Med Imaging Graph. Author manuscript; available in PMC 2013 July 01.

Table 1

The 14 clinical parameters and data distribution collected for decision-making regarding CTD for pneumothorax.

Parameter	Description	Min	Max	Mean	Std. Dev.
Type	Whether pneumothorax is occult or	overt Overt: 19; Occult: 52			
Linear size (mm)	Maximum thickness of the pneumothorax	1.70	86.40	16.55	16.99
Position	Whether the pneumothorax is located in the anterior, posterior, or lateral region	Anterior: 54; Posterior: 5; Lateral: 12			
Score	The score of pneumothorax is calculated based upon the linear size	10	106.40	25.69	18.27
Volume (cc)	Volumetric size of the pneumothorax	0.02	1028.36	101.92	196.75
Mech	Cause of injury: fall, motor vehicle accident, gunshot, etc.	MVC: 33; Fall: 22; Gunshot and struck: 2, others: 3			
Contusion (0–5)	Degree of lung contusion out of 6	0	5	1.92	1.57
RibFXn	Rib fractures (number of fractures)	0	12	3.46	3.22
RibFxX01	0 = no rib fracture, 1 = rib fracture (any number)	No rib fracture: 18; Rib fracture: 53			
Systolic BP (mm HG)	Systolic blood pressure	65	200	128.36	27.71
HR (beats per minute)	Heart rate	59	160	92.04	23.72
Hematocrit (Hct) (%)	Red blood cell percentage	28.70	50.80	39.54	4.59
CO_2 (mEq/L)	Blood CO_2 level	12.30	33.30	24.32	3.40
PPV	Whether treated by positive pressure ventilation (PPV)	Treated: 39; Not treated: 32			

Table 2

SVM and GA parameters used for searching the optimal parameter combination.

	Name of parameter	Values of parameter
GA algorithm	Number in population	16
	Number of iterations	1000
	Mating	Roulette-wheel selection
	Cross-over type	2 points
	Mutation probability	10%
SVM classifier	SVM type	C_SVM
	Kernel type	RBF (radial basis function)
	γ (gamma)	0.15
	Cost	20

Table 3

Performance of the 100-best parameter combinations in the four studies, measured by the Az value of the ROC curve.

	Mean	95% CI	Min.	Max.	Std. Dev.
Study I: 14 parameters	0.905	0.904–0.906	0.897	0.931	0.007
Study II: 13 parameters	0.849	0.847–0.851	0.835	0.885	0.011
Study III: 11 parameters	0.732	0.725–0.738	0.690	0.840	0.035
Study IV: 12 parameters	0.856	0.855–0.859	0.840	0.906	0.010

Table 4

Statistical size of the 100-best parameter combinations in the four studies.

	Mean	Std. Dev.	Median
Study I: 14 parameters	4.39	1.30	4
Study II: 13 parameters	4.71	1.73	5
Study III: 11 parameters	6.66	1.54	7
Study IV: 12 parameters	5.78	1.29	6

Table 5

The *p*-value for the *F*-test of pairwise comparison of the four studies.

	Study I	**Study II**	**Study III**	**Study IV**
Study I	N/A	<.001	<.001	<.001
Study II	N/A	N/A	<.001	.324
Study III	N/A	N/A	N/A	<.001
Study IV	N/A	N/A	N/A	N/A

Table 6

The best performance (*Az* value) with 1, 2, 3, and 4 parameters in Study I.

Rank	Performance	Parameter combination
1	0.931	Volume, Score, Hematocrit
2	0.928	Volume, HR, Systolic BP, Hematocrit
18	0.912	Volume, Hematocrit
78	0.899	Volume